

Enhanced light emission in photonic crystal nanocavities with Erbium-doped silicon nanocrystals

Maria Makarova,^{1,a)} Vanessa Sih,¹ Joe Warga,² Rui Li,² Luca Dal Negro,² and Jelena Vuckovic¹

¹Department of Electrical Engineering, Stanford University, Stanford, California 94305, USA

²Department of Electrical and Computer Engineering, Boston University, Boston, Massachusetts 02215, USA

(Received 7 February 2008; accepted 1 April 2008; published online 22 April 2008)

Photonic crystal nanocavities are fabricated in silicon membranes covered by thermally annealed silicon-rich nitride films with Erbium-doped silicon nanocrystals. Silicon nitride films were deposited by sputtering on top of silicon on insulator wafers. The nanocavities were carefully designed in order to enhance emission from the nanocrystal sensitized Erbium at the 1540 nm wavelength. Experimentally measured quality factors of ~ 6000 were found to be consistent theoretical predictions. The Purcell factor of 1.4 was estimated from the observed 20-fold enhancement of Erbium luminescence. © 2008 American Institute of Physics.

[DOI: 10.1063/1.2916711]

Silicon (Si)-based light sources compatible with mainstream complementary metal-oxide semiconductor technology are highly desirable because of their low manufacturing cost relative to III/V semiconductors and because they will enable monolithic integration with electronic components on the same Si platform. Here, we explore the enhancement of erbium (Er) emission coupled to photonic crystal (PC) nanocavities fabricated in a material consisting of silicon nanocrystals (Si-nc) embedded in silicon nitride¹⁻⁵ deposited on a silicon on insulator (SOI) wafer. These materials are of particular interest because Si-nc in silicon nitride can efficiently excite Er ions by fast nonradiative energy transfer, which could potentially lead to a Si-based optical amplifier with reduced pumping threshold. In addition, the Er emission at the wavelength of 1.54 μm is particularly suitable for high-density Si integration and is of strategic importance in fiber-based optical communication.

Confining luminescent material in an optical nanocavity increases its efficiency by restricting the resonant wavelength to a directed radiation pattern that can be effectively collected, and by reducing the radiative lifetime of the on-resonance emitters while suppressing off-resonance emission through the Purcell effect.^{6,7} We use two-dimensional (2D) PC nanocavities because of their high quality factor (Q) values and small mode volumes (V), since both are necessary for the Purcell effect. Previously, Si-nc-sensitized Er emission has been coupled to 2D PC slab modes to enhance vertical emission, but no cavity structures were studied.⁸

Two different approaches were considered for the photonic crystal cavity design for enhancing the spontaneous emission of Erbium embedded in the silicon-rich silicon nitride (SRN) film. In the first approach, a SRN film constituted the entire PC membrane, which is similar to the structures we have previously fabricated to enhance emission at 700 nm from Si-nc.⁹ In the second approach, a hybrid structure using a thinner SRN layer on a Si membrane was used. Three-dimensional finite difference time-domain calculations were used to estimate Q , V , and the average Purcell effect for

the single-hole (S1) defect cavity shown in Fig. 1(a). The results for three different membrane designs are summarized in Fig. 1(c). In the simulations, 20 points were used per period a ; the membrane thickness was $0.75a$ and for hybrid structures, the SRN thickness was $\frac{1}{3}$ of the total; and Si and SRN refractive indices were 3.45 and 2.4, respectively. The reported Q s correspond to the out of plane losses, and are converging to the total Q factor as the number of PC layers surrounding the cavity increases. Figure 1(a) shows the electric field magnitude for the high Q x -dipole mode, and Fig. 1(c) shows the field distribution for the membrane in cross section for each design. Si-based membranes have 2.75 times higher Q factors as expected due to greater refractive index contrast, and despite the electric field maximum falling outside the SRN layer, the average Purcell effect is still 2.5 times greater for the hybrid Si/SRN structure. The Purcell factor F_{avg} was spatially averaged over the SRN layer in the area indicated by the white circle in Fig. 1(a). We did not

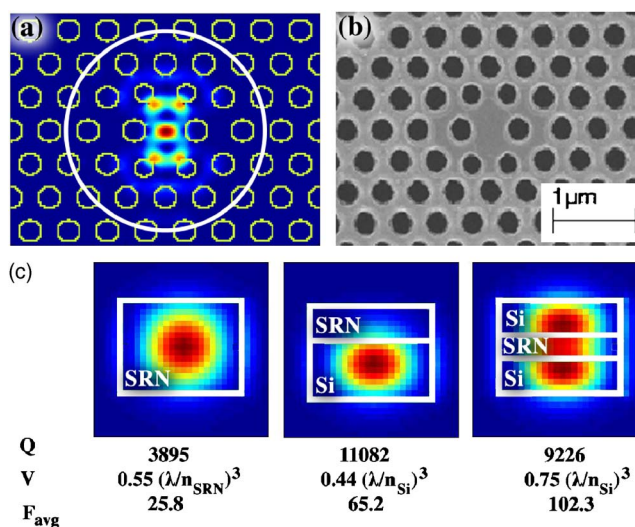


FIG. 1. (Color online) (a) Electric field magnitude of the x -dipole mode of a modified S1 defect cavity in the center of the slab and (c) in cross section for SRN, Si/SRN, and Si/SRN/Si membrane designs. (b) Scanning electron microscope image of the fabricated photonic crystal cavity.

^{a)}Electronic mail: makarova@stanford.edu.

average over dipole orientation because, experimentally, we can collect only the emission polarized along the mode. Given the difference in the expected performance, we fabricated cavities with hybrid Si/SRN membranes. Even higher enhancements are expected from cavities fabricated from symmetric Si/SRN/Si membranes because the electric field is stronger in the SRN layer, as seen in Fig. 1(c), but they require a different growth process.

We have fabricated Er-doped Si-nc embedded in amorphous silicon nitride matrices by radio frequency (rf) magnetron cosputtering of SRN followed by thermal annealing. The sputtering was performed in a Denton Discovery 18 confocal-targets sputtering system. The annealing process induces a precipitation transformation where the metastable Si-rich dielectric film decomposes into two stable phases: Si clusters and a matrix which, depending on Si supersaturation and annealing temperature/time, can be closer in composition to the equilibrium (stoichiometric) composition. In order to induce precipitation of small Si clusters and activate Er emission via efficient nonradiative energy transfer, the Si-nc films were annealed using a standard rapid thermal annealing furnace in N_2/H_2 forming gas (5% hydrogen) for 10 min at 700 °C. Under these conditions, TEM analysis demonstrates the nucleation of crystalline Si clusters with 2 nm diameter.^{1,4,5}

We have coupled Er-doped Si-nc to photonic crystal nanocavities by the following fabrication process. First, we deposited 100 nm of SRN on an SOI substrate with the top Si layer thinned down to 200 nm by successive oxidation and wet etching. Then, photonic crystal structures were defined by electron beam lithography in ZEP resist. The pattern is transferred into the SRN and Si layers by a magnetically enhanced reactive ion etch with Cl_2 and HBr gases. Finally, the underlying oxide layer is removed using hydrofluoric acid to form PC membranes. We fabricated numerous PC cavity membranes with S1 and Linear three-hole-defect (L3) cavities. A fabricated S1 cavity with a periodicity of 430 nm is shown in Fig. 1(b).

The structures are characterized using a confocal micro-photoluminescence setup with 473 nm excitation wavelength. This excitation is nonresonant with Er direct absorption and, therefore, it enables the unambiguous study of the Si-nc-sensitized Er emission enhanced by the photonic structures. The excitation laser is focused to $\sim 5 \mu m$ spot. Photoluminescence (PL) spectra taken with 1.71 mW pump power from modified S1 defect PC cavities with varying hole radii and from an unpatterned region, used as a reference, are shown in Fig. 2, where up to 20-fold enhancement of the Er emission in the PC cavities is evident. Coupling to both S1 and L3 cavities was observed with quality factors of 3230 and 1660, respectively, with 1 mW pump power. Polarization-resolved measurements verify coupling to the X-dipole mode of the S1 cavities and the Y-polarized fundamental mode of the L3 cavities. The maximum Q factor of 6380 was observed for a S1 cavity using 2.5 μW pump power.

Figures 3 and 4 show the evolution of the PC resonance with increasing pump power. Interestingly, the resonance Q factor decreases by a factor of 2 as the pump power is increased from 2.5 μW to 1.7 mW. The observed redshift of the resonance indicates a refractive index decrease as expected from sample heating. Q factors probably diminish because the refractive index contrast necessary for good con-

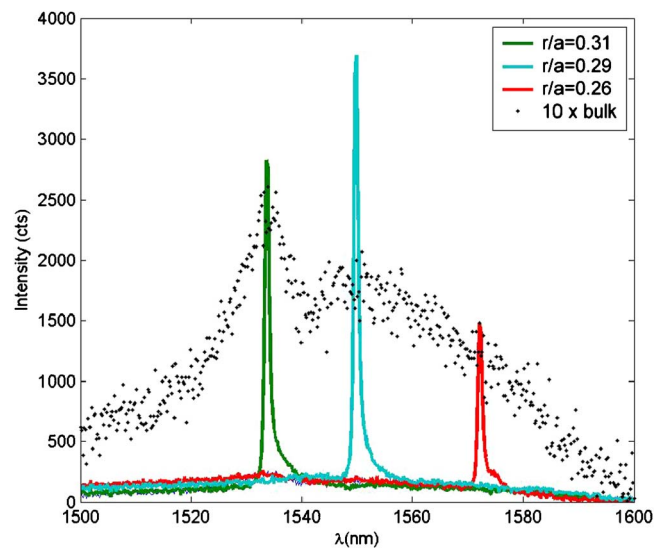


FIG. 2. (Color online) Room-temperature photoluminescence spectra from PC cavities with varying hole radii which span the Er spectrum, and the unprocessed wafer (bulk) emission shown at 10 times for clarity.

finement is degraded. Photoluminescence intensity saturation is observed for both cavity coupled and uncoupled emission. At pump powers below 0.5 mW, the PL intensity behavior of coupled and uncoupled emitters appears almost the same. With the Purcell effect shortening the radiative lifetime, we would expect the cavity to saturate at a higher intensity. It is possible that this effect is masked by a stronger pump power absorption in the PC cavity and by the Q factor falling with increasing pump power. Another possibility is that the radiative recombination rate is much lower than the nonradiative rate and increasing it through the Purcell effect does not significantly affect the overall lifetime of the excited state. This is especially a concern at higher pump powers where cooperative Er upconversion is possible. Direct lifetime measurements are necessary to unambiguously determine to what extent the Er radiative lifetime coupled to the cavity is shortened by the Purcell effect.

However, it is still possible to estimate the actual Purcell effect from the experimental data on the emission enhance-

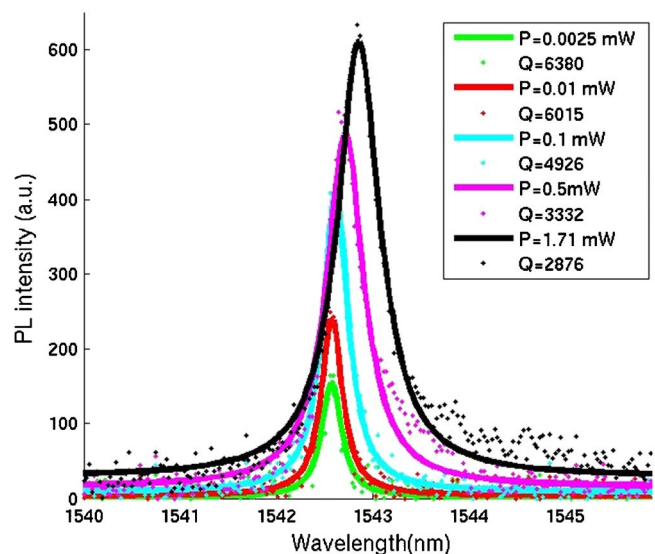


FIG. 3. (Color online) Pump power dependence of a PC resonance. The solid lines are Lorentzian fits.

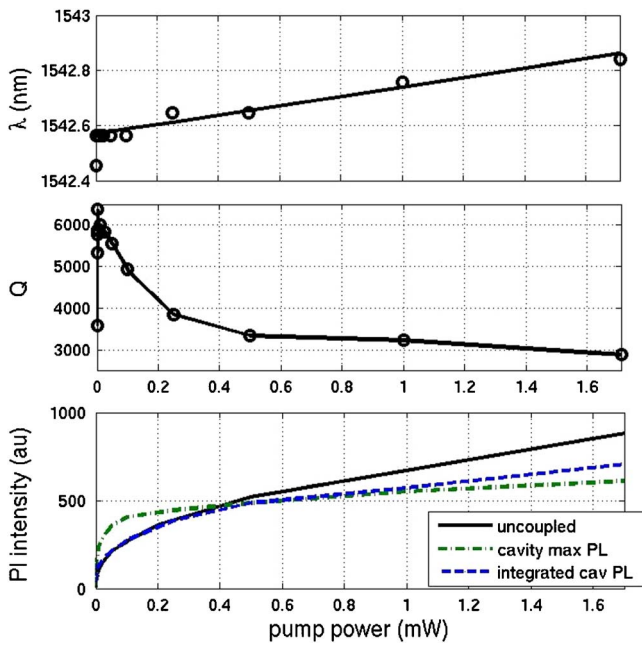


FIG. 4. (Color online) Resonant wavelength, cavity quality factor, and PL intensity dependence on pump power. The intensities are scaled for easier comparison.

ment compared to the unpatterned film and from the calculated electric field distribution inside the cavity. There are two reasons for observing enhanced PL emission from the cavity region—Purcell effect and improved collection efficiency due to directed radiation from the cavity. The collection efficiency of the S1 cavity X-dipole mode with 0.2 numerical aperture (NA) is estimated at 2.4% from the Fourier transform of the field just above the cavity.¹⁰ In comparison, the collection efficiency from the smooth SRN film is given by $1/2 \int_0^{\arcsin(\text{NA}/n_{\text{SRN}})} \sin(\theta) d\theta = 0.17\%$. Thus, the expected enhancement due to the improved collection efficiency is $2.4/0.17 = 14$. Since we observed a 20-fold overall enhancement, we estimate that the average Purcell factor is around $20/14 = 1.4$. Another way to estimate the average Purcell factor is to use the measured Q factor, calculated mode volume, and calculated average electric field magnitude in the SRN film over the excitation area. The Purcell factor

$$F_{\text{avg}} = \frac{3}{4\pi^2} \frac{n_{\text{Si}}}{n_{\text{SRN}}} \frac{Q}{V(n_{\text{Si}}/\lambda_0)^3} \psi,$$

with

$$\psi = \sum_i \frac{|E_i|^2}{|E_M|^2},$$

where the sum is over the excited volume of SRN film, and E_M is the electric field where $n^2|E|^2$ is maximum. Note that the term accounting for the emitter dipole and electric field alignment is omitted from the above equation because we recorded only the emission polarized with the cavity mode. The expected $F_{\text{avg}} = 3$, given the experimental Q of 2876, ψ of 0.0043 calculated over the $5 \mu\text{m}$ excitation spot, and V of $0.44 (\lambda_0/n_{\text{Si}})^3$.³ This estimate of 3 is quite consistent with the earlier estimate of 1.4, which may be lower because it depends on how well the collection optics is aligned with the cavity. Note that the above analysis was done for high pump

powers where the cavity Q factor is degraded. At low pump power, where Q is 6380, the average Purcell factor should be on the order of 3 to 7, but we are not able to directly estimate it from emission enhancement because at low excitation, the PL signal from the smooth film is at the noise level.

We observe coupling of Er emission to Si-based PC cavities over its entire luminescence region. The optimized S1 defect cavity presented here has a maximum measured Q factor of 6380 at low pump power, which favorably compares with 11 082, which is theoretically predicted. We observe up to 20-fold enhancement of emission coupled to the PC cavity at high pump power and estimate 44-fold enhancement at low pump power. The maximum possible Purcell factor is $F = 665$ for Er emitters aligned with the highest field in the nitride layer in the characterized S1 cavity. The experimental value is lower because it is a spatial average of excited Er emitters distributed around the cavity. Therefore, the experimental value strongly depends on the excitation spot size and PL collection area. If we restrict the collected PL signal to a $2 \mu\text{m}$ diameter area around the cavity instead of $5 \mu\text{m}$, we expect to improve the experimentally observed enhancement by a factor of 7. So with our current cavities, we should be able to observe Purcell factors of around 21–49 by spatially filtering PL. Further improvements can be achieved by going to a symmetric structure, such as shown in Fig. 1(c), where the SRN layer is in the center of the membrane and has a much higher overlap with the field. These results demonstrate that the Er emission sensitized by Si-nc can be dramatically enhanced by coupling with photonic crystals nanocavities, paving the way to the demonstration of optical amplifiers entirely compatible with Si technology.

This work was partially supported by MARCO Interconnect Focus Center, U.S. Air Force Office of Scientific Research (AFOSR) program supervised by Dr. Gernot Pomrenke, and the U.S. Air Force MURI program on “Electrically Pumped Silicon-Based Lasers for Chip-Scale Nanophotonic Systems” supervised by Dr. Gernot Pomrenke. The fabrication was done in part at the Stanford Nanofabrication Facility of NNIN. M.M. is also supported by the Intel Fellowship.

¹N. M. Park, C. J. Choi, T. Y. Seong, and S. J. Park, *Phys. Rev. Lett.* **86**, 1355 (2001).

²L. Dal Negro, J. H. Yi, L. C. Kimerling, S. Hamel, A. Williamson, and G. Galli, *Appl. Phys. Lett.* **88**, 183103 (2006).

³L. Dal Negro, J. H. Yi, J. Michel, L. C. Kimerling, S. Hamel, A. Williamson, and G. Galli, *IEEE J. Sel. Top. Quantum Electron.* **12**, 1628 (2006).

⁴L. Dal Negro, S. Hamel, N. Zaitseva, J. H. Yi, A. Williamson, M. Stolfi, J. Michel, G. Galli, and L. C. Kimerling, *IEEE J. Sel. Top. Quantum Electron.* **12**, 1151 (2006).

⁵L. Dal Negro, R. Li, J. Warga, S. Yerci, S. Basu, H. Hamel, and G. Galli, in *Silicon Nanophotonics: Basic Principles, Present Status and Perspectives*, edited by L. Khriachtchev (World Scientific, Singapore, in press).

⁶E. M. Purcell, *Phys. Rev.* **69**, 681 (1946).

⁷J. Vuckovic, C. Santori, D. Fattal, M. Pelton, G. S. Solomon, and Y. Yamamoto, in *Optical Microcavities*, edited by K. Vahala (World Scientific, Singapore, 2004).

⁸M. Galli, A. Politi, M. Belotti, D. Gerace, M. Liscidini, M. Patrini, L. C. Andreani, M. Miritello, A. Irrera, F. Priolo, and Y. Chen, *Appl. Phys. Lett.* **88**, 251114 (2006).

⁹M. Makarova, J. Vuckovic, H. Sanda, and Y. Nishi, *Appl. Phys. Lett.* **89**, 221101 (2006).

¹⁰J. Vuckovic, M. Loncar, H. Mabuchi, and A. Scherer, *IEEE J. Quantum Electron.* **38**, 850 (2002).